ACS APPLIED POLYMER MATERIALS

pubs.acs.org/acsapm Article

Polybutadiene Click Chemistry: A Rapid and Direct Method for Vat Photopolymerization

Levi M. J. Moore,* Van Michael Q. Saludo, Oliver H. Grasdal, Kayleen M. Smith, Thomas J. Kolibaba, Jacob C. Marcischak, Jason P. Killgore, Jeremy J. Snyder, Gregory R. Yandek, and Kamran B. Ghiassi

Cite This: https://doi.org/10.1021/acsapm.3c01601 Read Online

ABSTRACT: Thiol−ene click chemistry was utilized to cross-link unmodified commercial liquid polybutadiene, and complex geometries were 3D printed using vat photopolymerization. PB homopolymer contains pendent reactive moieties inherent to its synthesis which were used as cross-linking sites in a photosensitive resin without copolymerization or postpolymerization modification of the PB to include conventional photocurable moieties such as acrylates. Thiols were found to preferentially react with pendent olefinic units, and the mechanical properties of cross-linked specimens generally behaved as expected, that is, an increase in the cross-link density led to an increase in tensile stress but a decrease in strain at break. Resins were downselected for printability and working curves were obtained, showing evidence of a "dark cure" attributed to the thiol−ene reaction's relative insensitivity to oxygen. Objects with challenging structures were printed by using commercial digital light processing printers..

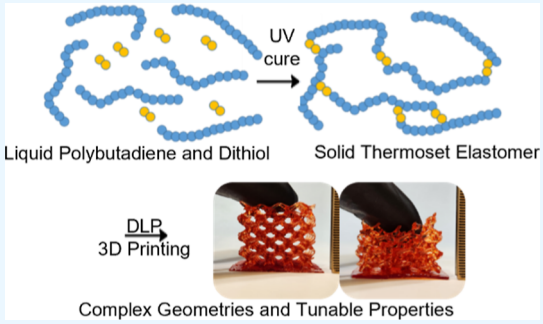

KEYWORDS: *polybutadiene, thiol−ene, click chemistry, elastomer, vat photopolymerization*

1. INTRODUCTION

Since its inception, additive manufacturing (AM), also known as 3D printing, has been widely used in rapid prototyping and model making. AM has shown remarkable success in the acceleration of product development times due to its ability to rapidly produce prototypes without needing or waiting for the expensive tooling employed in conventional manufacturing. AM has become so prevalent that consumer-grade desktop 3D printers are now available to hobbyists regularly for under $300. Significant advances in AM technologies have enabled printing of metals, ceramics, and plastics with complex geometries which are not possible through conventional casting or injection molding. This greatly expands the realms of possibility for unconstrained, advanced, and complex designs.

An area that has been relatively underexplored is the development of rubbery materials for 3D printing. Fused filament fabrication and direct ink write have been used to print flexible materials such as thermoplastic polyurethane,[1,2] and compounded rubber,[3] but due to the inherent mechanical properties of elastomers, these techniques remain limited for a wide range of soft materials compared to the possibilities offered via vat photopolymerization (VP).[4] In addition to the growing number of commercial VP resins with undisclosed formulations, academic research has been prolific in recent years,[3] using VP techniques to print elastomers such as high molecular weight latexes[5] and polysiloxanes with high stretchability.[6]

Although the soft materials listed above are indeed significant advancements in 3D printing, there is a need to expand the library of available materials that can be printed, especially to include commodity polymers, such as diene rubbers. These elastomeric polymers offer properties not available with the current soft materials utilized in 3D printing. Such materials are widely used as gaskets, seals, bushings, and so forth in myriad applications from automotive to aerospace due to their resilience and tolerance to deformation. The ability to print rubber materials can potentially extend the service lifetimes of equipment by enabling the production of discontinued elastomeric gaskets, seals, and bushings on an as-needed basis, supplying parts that are no longer economically feasible to mass produce. This thrust of research would also expand the library of materials to produce elastomeric and soft-touch materials in advanced manufacturing.

Conventional thermal curing of diene rubbers is generally accomplished through the vulcanization process, where

Received: July 21, 2023
Accepted: September 25, 2023

polydienes [e.g. polyisoprene or polybutadiene (PB)] are compounded with elemental sulfur and cure catalysts, and catalysts are cured at elevated temperature to yield a cross-linked, vulcanized article.[7] UV-light-promoted curing is necessary for VP though, and to date, the majority of UV-curable chemistries that have made use of polydienes or their derivatives have required installation of (meth)acrylate groups on telechelic starting materials.[8,9] These modifications add significant processing steps and undesirable material expense. As an alternative functionalization technique, the radical thiol−ene reaction has been successfully employed to functionalize PB with several functional thiols.[10] The 1,2-*vinyl* addition structural moieties were shown to react strongly with thiols, leading to the anti-Markovnikov reaction product. There are few other reports on the use of thiol−ene chemistry as a method of cure for polydiene rubber materials, although this area is relatively unexplored.[11]

Liquid PBs are commercially available and are used as reactive plasticizers in vulcanized rubber compounding.[12] Low molecular weight polymers (ca. 5500−8000 g mol^{-1}, η = 0.6−1.5 Pa·s) are relatively low viscosity liquids, while higher molecular weight liquid polymers are much more viscous (ca. 26,000 g mol^{-1}, η = 40 Pa·s).[13] VP processes typically necessitate resin viscosities < 10 Pa·s to be feasible without unconventional blade deposition of resins.[14] As such, the liquid nature and tolerable viscosities of relatively low molecular weight PBs make them favorable candidates for VP. Previous efforts to use thiol−ene chemistry for VP have shown its utility to print highly stretchable silicones[6] and acrylate-modified liquid hydrocarbon polymers.[8,15] Low molecular weight unmodified PB has been shown to be UV-cross-linkable,[16] curing the liquid PB using a widely available trithiol to form thin films of cured rubber using a direct-write technique. There are only a few commercially available polythiols, and those with a functionality greater than two contain highly polar ester groups, making them immiscible with the nonpolar PB. This immiscibility leads to phase separation, poor light penetration due to scattering, incomplete cure, and diminished mechanical properties.

This study characterizes the cross-linking reaction between PB and a completely miscible thiol in the UV-promoted thiol−ene reaction, without the need for any additional chemical modification to the parent PB prepolymer. Mechanical properties of cross-linked PBs of varied molecular weights are reported using a commercially available dithiol that is miscible with polybutadiene. Candidate formulations were downselected and printed using VP in a commercial digital light processing (DLP) printer. The best candidate PB resins were capable of being directly printed into complex geometries without the use of a scaffold or volatile additives, enabling dimensional stability and reproducibility.

2. MATERIALS AND METHODS

2.1. Materials and General Considerations. LBR-302 (M_n = 5500 g mol^{-1}, η = 0.6 Pa·s), LBR-307 (M_n = 8000 g mol^{-1}, η = 1.5 Pa·s), and LBR-305 (M_n = 26,000 g mol^{-1}, η = 40 Pa·s) were obtained from Kuraray.[13] For clarity in nomenclature and distinction in molecular weight, LBR-302, LBR-307, and LBR-305 will be referred to as PB-5k, PB-8k, and PB-26k, respectively, in the remainder of the report. Diphenyl(2,4,6-trimethylbenzoyl)phosphine oxide (TPO), 1-decanethiol, and 3,6-dioxa-1,8-octanedithiol (ODT) were purchased from TCI. Bis(2-ethylhexyl) adipate, Oil Red O, and tetramethylsilane (TMS) were obtained from Sigma-Aldrich. All materials were used as received. A FlackTek SpeedMixer DAC 600 FVZ instrument was used for mixing. Nuclear magnetic resonance (NMR) experiments were performed on a Bruker AVANCE III HD 400 MHz spectrometer using $CDCl_3$ as the solvent. ^{1}H spectra were referenced internally to the residual solvent. Negative molds for tensile testing specimens were 3D printed using a Formlabs Form 2 and clear resin. The negatives were used to cast molds for tensile specimens using a SilPak R2364 RTV silicone. Tensile specimens were cured in a Formlabs Form Cure instrument with a maximum output intensity of approximately 1 mW/cm^2.

2.2. Reaction of PB with Monothiol for NMR Analysis. 1-Decanethiol (1.9 g, 10.9 mmol), TPO (42 mg, 121 μmol), and TMS (240 mg) were combined in a scintillation vial and heated with agitation until a homogeneous mixture was obtained. PB-5k (2.5 g, 45.5 mmol double-bond moieties) was added, and the vial was mixed in the SpeedMixer for 2 min at 2300 rpm, followed by irradiation without stirring for 10 min at room temperature in a Formlabs Form Cure. The reaction product was notably more viscous than the initial mixture, although still liquid.

2.3. Preparation of Photoresins. Photoinitiator (TPO) and thiol (ODT) were added to a polypropylene mixing cup that was subsequently agitated while heating until a homogeneous solution formed. If required, dye (Oil Red O), and/or plasticizer was then added and mixed again. The liquid PB was then weighed into a mixing cup and mixed in a dual axis centrifuge for 2 min at 2300 rpm. For example, to prepare the PB-5k/10SH formulation for UV-cast tensile articles, 58 mg of TPO and 8.29 g of ODT were added to a polypropylene mixing cup which was agitated with heating until the TPO dissolved into the ODT. PB-5k (50.0 g) was then measured into the mixing cup and mixed at 2300 rpm in a dual axis centrifuge. To prepare the photoresin for VP, the abovementioned procedure was followed, but the photoabsorber, Oil Red O (12 mg), was added to the solution of TPO and ODT and agitated to dissolve before the addition of the liquid polybutadiene. Detailed formulations for all photoresins used to prepare tensile samples (without photoabsorber or plasticizer) are presented in the Supporting Information in Table S1.

2.4. Mechanical Testing. Cast photocured samples were prepared by pouring undyed photoresin into a silicone tensile specimen mold based on ASTM D412 Die C dimensions and cured in a Formlabs Form Cure for 10 min at room temperature. Tensile properties were tested on an Instron 3340 single-column test frame with a 500 N load cell at a crosshead speed of 51 mm min^{-1}. Modulus values were obtained from the slope of the stress−strain curve between 0 and 5% strain. Shore A values were measured using an Insize Shore A durometer in an Insize testing stand.

2.5. Vat Photopolymerization. Working curve measurements of cure depth *versus* light exposure were performed in-printer by projecting 16 squares (1 mm × 1 mm) one at a time with incrementally longer times for each projection onto a silanized glass coverslip[17] placed on an Asiga Max X27 405 nm DLP printer (Asiga, Alexandria, NSW, Australia). The glass coverslip (no. 1 Corning cover glass, purchased from Sigma-Aldrich) was functionalized with 3-(trimethoxysilyl)propyl methacrylate (98%, Sigma-Aldrich) and located over the screen, in place of the typical FEP window.[17] For 7 mW cm^{-2} irradiance working curves, each square was projected for 5 s longer than the last (*i.e.*, square 1 was projected for 5 s, square 2 for 10 s, square 16 for 80 s) and for 30 mW cm^{-2} irradiance, each square was projected with 1 s increments. Coverslips were then prepared by pipetting photoresin to a depth of >1 mm, allowing the surface tension of the resin to hold the pool in place on the functionalized slide. UV−vis spectra were acquired on a NanoDrop One variable path length spectrophotometer (Thermo Fisher Scientific, Waltham, MA, USA).

3D printing experiments were performed on a mUVe3D DLP Pro (mUve 3D, Grand Rapids, MI, USA) with an intensity of ca. 7 mW cm^{-2} or an Asiga Max X27 printer with its irradiance set to 30 mW cm^{-2}. Standard tessellation language files were sliced to a layer thickness of t_{layer} = 100 μm. The first two layers of each print received 50 s (15 s for the Asiga printer) of irradiation to ensure adhesion to the build plate. Subsequent layers were exposed for 20 s (5 s for the

https://doi.org/10.1021/acsapm.3c01601
ACS Appl. Polym. Mater. XXXX, XXX, XXX−XXX

Table 1. Tabulated Mechanical Properties of the UV-Cast Formulations[a]

polymer	SH/chain	Th. MWBXL	shore A hardness	modulus (MPa)	ultimate tensile stress (UTS) (MPa)	strain at break (%)
PB-5k	5	1100	34 ± 2	0.68 ± 0.04	0.19 ± 0.05	33.3 ± 8.9
	10	550	62 ± 2	2.64 ± 0.06	0.68 ± 0.13	29.2 ± 6.2
	15	367	73 ± 1	4.15 ± 0.22	0.80 ± 0.15	20.6 ± 3.4
PB-8k	5	1600	32 ± 1	0.63 ± 0.07	0.20 ± 0.03	42.6 ± 7.4
	10	800	58 ± 2	1.04 ± 0.16	0.32 ± 0.06	38 ± 14
	15	533	67 ± 3	3.51 ± 0.07	0.80 ± 0.13	26.1 ± 5.2
PB-26k	5	5200	24 ± 1	0.46 ± 0.11	0.28 ± 0.04	109 ± 33
	10	2600	49 ± 2	1.06 ± 0.13	0.36 ± 0.07	43 ± 11
	15	1733	58 ± 2	3.55 ± 0.06	0.92 ± 0.21	30.3 ± 8.4

[a]Detailed formulations are presented in the Supporting Information. Error values represent one standard deviation from a minimum of five replicates.

Asiga printer). Between layers, the LED was shut off for 1.9 s and the build plate was lifted 5 mm from the build plane with a peel speed of 0.25 mm s^{-1}, and retracted (*i.e.*, brought back toward the print window) at 1 mm s^{-1} to its new position before projecting the next layer. All prints were performed with 50−60 g of the respective photoresin (formulations shown in Table 2). Parts were removed from the build plate by a razor blade. On some prints, a very weak gel formed around the top of the part which was removed manually with a plastic spatula.

Table 2. Photopolymer Resin Formulations Used for Printing[a]

polymer	mass polymer (g)	mass ODT (g)	mass TPO (g)	mass Oil Red O (g)	mass plasticizer (g)
PB-5k	50	8.286	0.583	0.012	
PB-8k	50	5.697	0.557	0.011	
PB-26k	35	1.227	0.512	0.010	15

[a]Resin based on PB-26k required a 50 s layer cure time.

3. RESULTS AND DISCUSSION

3.1. Reactivity of Thiol with PB. Previous reports have shown that monothiols react with high-vinyl PB to yield ring-closing and the monothiol addition products.[10] In the realm of AM, however, the thiol−ene addition to form a cross-linked system is largely uncharacterized. With regard to liquid polybutadiene, the potential thiol−ene cross-linking is more complex because the polymers generally consist of a mixture of trans/cis/vinyl constituents with a respective ratio of approximately 60:20:20 (*vide infra*). The vinyl group is understood to react with thiols to yield an addition product,[10,18−20] but there are fewer reports that characterize the reactivity of the other two moieties (*i.e.*, the 1,4-*cis* and 1,4-*trans* internal constituents).[21] To probe this, an amount of 1-decanethiol sufficient to add to roughly one-fourth of the double bonds in the polymer was reacted with PB-5k. TPO was used as the photoinitiator, and TMS was used as an internal standard to compare changes in peak area of the reacting moieties. The reaction was performed without solvent to mimic the cross-linking conditions experienced in a formulated resin.

The NMR spectra of the reaction mixture are shown in Figure 1, before (a) and after (b) irradiation at 405 nm for 10 min. Before irradiation, all resonances (labels A−K) consistent with the polymer and thiol are apparent and distinct. After irradiation, resonances from the thiol moiety (labels G−K) broaden, consistent with the addition to a polymer molecule. A

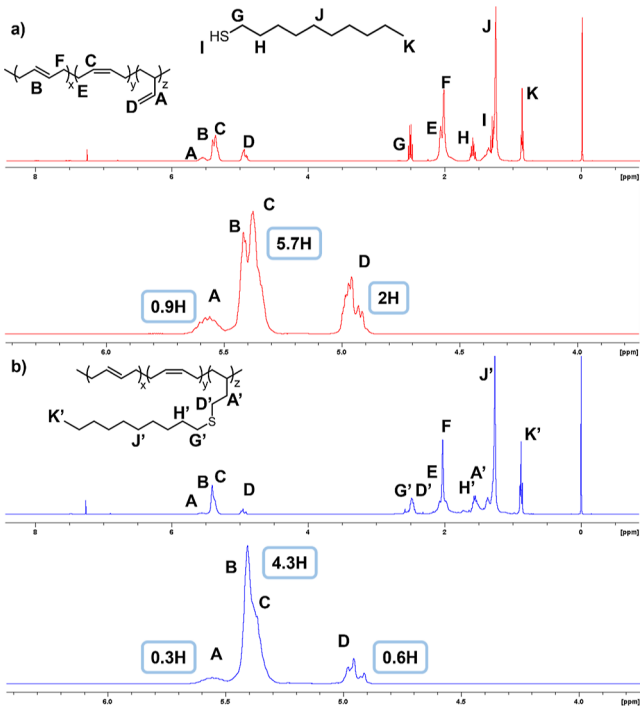

Figure 1. NMR spectra of the reaction of PB with 1-decanethiol before (a) and after (b) UV irradiation, showing starting reactants and a representative addition product. The olefinic region of the spectrum is detailed below each full spectrum. Letters A−K represent proton assignments. Full spectra with integrals are presented in the Supporting Information.

representative addition product is shown in Figure 1b. In particular, the chemical shift around 2.5 ppm, which is assigned to the protons on the carbon alpha to the thiol group (Figure 1a, G), changes from a sharp quartet to a broad quartet. The triplet corresponding to the thiol proton disappears (Figure 1a, I), suggesting full conversion of the thiol to the addition product. The resonances at 4.9 and 5.6 ppm correspond to the pendent vinyl groups of the polymer (Figure 1a, D and A, respectively), and the resonances at 5.4 and 5.3 ppm correspond to the trans and cis moieties, respectively[22] (Figure 1a, B and C, overlapped). After irradiation, the areas of the vinyl peaks are reduced as well as the height of the peak for the *cis* isomer. This is consistent with signals in the aliphatic region as the peak corresponding to the cis moiety (Figure 1a, E) is reduced as well. Integration of peak areas compared to the TMS internal standard (see Supporting Information) shows that the resonance at 4.9 ppm corresponding to the terminal

https://doi.org/10.1021/acsapm.3c01601
ACS Appl. Polym. Mater. XXXX, XXX, XXX−XXX

protons on the pendent vinyl reduces in area from 2H to roughly 0.6H (Figure 1a,b, D). The resonance at 5.6 ppm corresponding to the proton on the secondary carbon in the vinyl group (Figure 1c, A) decreases in area by a similar factor, from 0.9H to 0.3H. The cis and trans olefinic peaks (B and C) overlap, so integration of each peak individually is not possible. Integrated together, a decrease in area of the overlapping cis and trans peaks is observed, from 5.7H to 4.3H. The concomitant decrease in the height of the cis peak illustrates consumption of the cis double bond. These decreases in area after UV irradiation show that both the cis and vinyl moieties react with thiols in the thiol−ene reaction, showing a preference for the thiol to react with vinyl groups over the cis groups. In addition, thiyl radicals have been shown to catalyze the isomerization of cis alkene moieties to trans moieties after addition and fragmentation.[21,23] This isomerization along with cross-linking together explain the decrease in area of the peak associated with the cis moiety. The trans constituents do not appear to preferentially react with the thiols under the same reaction conditions and irradiation times, though they are not precluded from reacting. In this system, the thiol preferentially adds to the vinyl moiety, followed by the cis moiety (which also isomerizes to the trans moiety by an addition−isomerization−fragmentation reaction), and trans moiety.

Representative ratios of trans/cis/vinyl units are presented in Figure 2, displaying the roughly 60% trans, 20% cis, and 20%

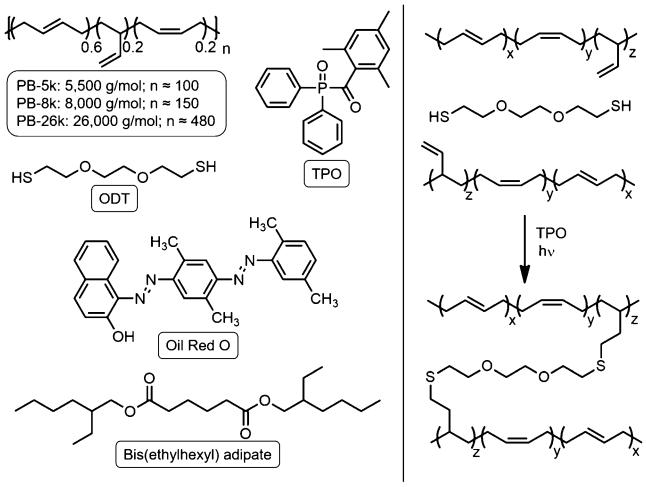

Figure 2. Materials utilized in this study to formulate photoresins (left) and structural depiction of cross-linking scheme (right).

vinyl common for liquid polybutadienes.[24] The preference of thiols to add to the pendent vinyl groups allows for formulation of VP photoresins with a precise number of cross-linking sites per chain, with a practical upper bound of reaction sites per chain being the number of vinyl units in the polymer plus the number of cis units based on the model study mentioned above. The use of a dithiol or higher, serving as a cross-linker, will result in network formation as it adds to the backbones of different polymer chains. In contrast to more conventional acrylate-based UV-curable resins, the cross-linking polythiol reacts in a step growth process rather than a chain growth polymerization process. In this study, all the polymers and thiol curative were capable of reaction at any point during the cross-linking process, ensuring high incorporation of reactive material into the cross-linked network. Acrylate-based resins can only react at active radical chain ends, and this reaction is inhibited by ambient oxygen, potentially reducing the amount of resin incorporated into the cross-linked network, which can inhibit mechanical properties. Additionally, acrylate functionalization of polymers generally incorporates a hydrolytically unstable ester linkage, none of which are present in the cross-linked networks presented here.

The materials selected for this study are presented in Figure 2 (left), along with a schematic depiction of a cross-linking reaction (right). A previous report by Bragaglia *et al.*, detailed the printing of a resin consisting of 5000 g mol^{-1} polybutadiene, trimethylolpropane tris(mercaptopropionate) (TMPMP) as the cross-linker, and ethyl(2,4,6-trimethylbenzoyl)phenylphosphinate (TPO-L) as the photoinitiator.[16] TMPMP is an attractive candidate for commercial-off-the-shelf formulation, as it has been the workhorse trithiol for thiol−ene formulation for more than a decade.[25] However, we found that TMPMP is immiscible with all of the PB varieties reported here due to its highly polar nature as a result of its ester moieties. Mixing of TMPMP, as well as its tetrafunctional analogue pentaerythritol tetrakis(3-mercaptopropionate) (PETMP), with PB leads to a white emulsion that rapidly phase separates after mixing. Attempts to cure a 5-mm thick tensile sample resulted in incomplete cures as light cannot penetrate completely into the mold. For this reason, other thiols that are miscible with PB were examined.

Commercially, the most accessible dithiol to use on a large scale is ODT. This compound has several advantages compared to other commercially available dithiols, such as relatively low cost, high molecular weight, and high boiling point. For comparison, the shorter chain compound 1,4-butanedithiol is less desirable due to its lower boiling point and higher vapor pressure, which yield a stronger, more noticeable, and unpleasant odor. To probe the similarity of the cross-linked polymer network topology to the previous report, a trithiol is desirable. Unfortunately, the only readily available thiols with a functionality greater than two are TMPMP and PETMP,[26] both of which are not miscible with PB due to their higher polarity. Therefore, ODT was used as the thiol curative of choice for formulation in this study.

3.2. UV-Cast Material Properties. Representative stress−strain curves of formulated PB resins of differing molecular weights cross-linked with varying thiol loadings are presented in Figure 3. Thiol loading corresponds to the number of thiol moieties per polymer chain present in the reaction mixture, and by extension the number of cross-linking sites per polymer chain. Tensile testing was performed using the ASTM D412 Die C geometry at a crosshead speed of 51 mm min^{-1}, with a minimum of five samples per formulation. Tabulated and graphically represented mechanical data are presented in Table 1 and Figure 4, respectively, along with calculated theoretical molecular weight between cross-links (MWBXL) in Table 1. The stress−strain curves show that all specimens exhibit brittle failure, consistent with a fully cross-linked polymer network.

Trends for stress and strain follow what is expected for increases in cross-linker concentration: strain at break decreases and UTS increases as concentration increases (and molecular weight between cross-links decreases). Tensile stress follows the familiar pattern of a marked increase in stress at failure as cross-linker concentration increases, with clear step changes from 5SH to 10SH to 15SH. However, in the PB-5k series the initial increase from 5SH to 10SH occurs as expected, but the step to 15SH is not statistically different from

https://doi.org/10.1021/acsapm.3c01601
ACS Appl. Polym. Mater. XXXX, XXX, XXX−XXX

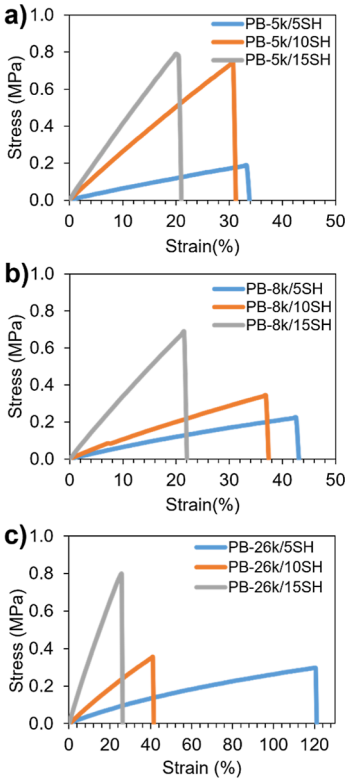

Figure 3. Representative stress−strain curves of UV-cast formulations with increasing cross-linker concentration (*i.e.*, moles thiol moiety per polymer chain). Formulations are based on PB-5k (a), PB-8k (b), and PB-26k (c). Note that the *x*-axis in (c) differs from (a,b).

the 10SH formulation. This is hypothesized to be due to only a small difference in the molecular weights between cross-links between the two formulations 550 g mol^{-1} *versus* 367 g mol^{-1} for the 10SH and 15SH formulations, respectively. This may be due to a threshold cross-link density around these values where additional cross-linking only leads to marginal increases in UTS.

The strain at break values for all formulations are lower than those for fully compounded rubber. This is most likely due to the prepolymers' lower molecular weight as well as potentially smaller effects like that of reinforcement through addition of filler. Rubber articles are generally produced through processing of high molecular weight polymer, typically on the order of 100,000−500,000 g mol^{-1}.[27] The highest molecular weight prepolymer in this study is only a fraction of this (PB-26k, ∼26,000 g mol^{-1}). The values for strain at break follow the expected trend of a higher concentration of cross-linker (lower molecular weight between cross-links) leading to a lower strain at break, though not all steps in formulation yield significant differences in the strain at break values. All the formulations are bound in the 20−40% strain at break except for the PB-26k/5SH formulation, which exceeds 100%. The molecular weight between cross-links value (∼5200 g mol^{-1}) for PB-26*k*/5SH is much higher compared to the rest of the formulations, which yields longer distances between cross-links that have the potential to extend further before breaking. The UTS values follow a similar expected trend, where a lower molecular weight between cross-links value leads to a higher UTS at break. All the 15SH formulations exhibit a similar value for their UTS, at around 0.8 MPa, with the UTS decreasing as less thiol cross-linker is added. The PB-5k/10SH formulation's UTS is higher than expected based on the results of the other two prepolymer formulations. However, this again can be explained by the relatively small difference in molecular weight between cross-links when comparing the 10SH and 15SH formulation.

The modulus and shore A hardness values all follow the expected trend as well, increasing with increasing cross-linker concentration. Both modulus and shore A hardness decrease as the molecular weight of the prepolymer increases, which is expected when the molecular weight between cross-links increases. The mechanical properties of the materials

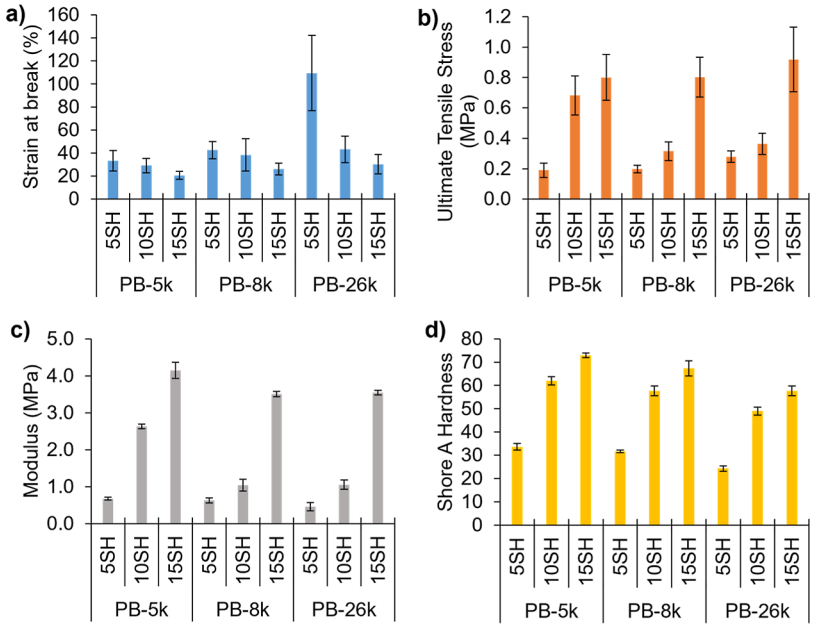

Figure 4. Strain at break (a), UTS (b), Young's modulus (c), and shore A hardness (d) of the UV-cast specimens. Error bars represent one standard deviation from a minimum of five replicates.

https://doi.org/10.1021/acsapm.3c01601
ACS Appl. Polym. Mater. XXXX, XXX, XXX−XXX

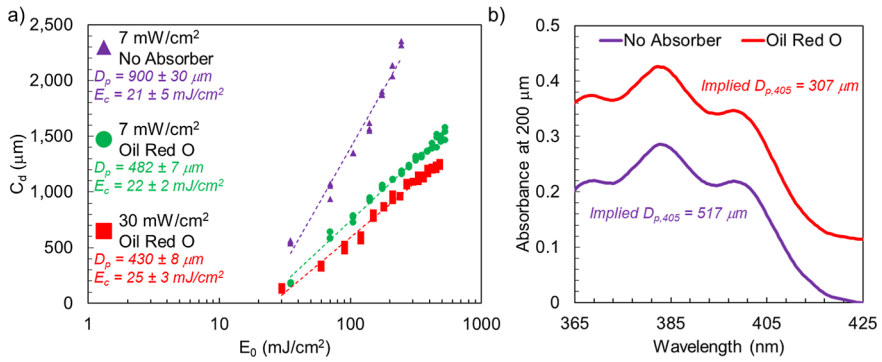

Figure 5. (a) Working curves for PB-5k/10SH resins with and without an Oil Red O absorber and at varying levels of irradiance. Extracted fit parameters indicate each resin's light penetration depth (D_p), and critical dose (E_c). (b) Short (200 μm) path length UV−vis spectra of PB-5k/10SH resin with and without the Oil Red O absorber.

characterized here span the range of those required by soft-touch applications. In particular, the shore A hardness varies from 24 to 73, bracketing commonly available elastomeric and rubbery resins. Other mechanical properties of traditionally formulated PB products are higher, but those include fillers which provide additional reinforcement to the cured polymer.[27]

3.3. DLP Printing. A resin formulation based on PB-5k was downselected to be the candidate for initial printing studies due to its low viscosity,[14] and proof-of-concept formulations were based upon the 10SH/chain formulation. Preliminary attempts to utilize an LCD printer with this resin system failed due to insufficient optical power (see Supporting Information). A DLP printer can attain substantially higher power outputs and thus can deliver a desired energy dose in significantly less time, reducing the effects of overexposure and overpolymerization. For this reason, a 405 nm DLP printer was chosen for subsequent printing studies. However, significant overpolymerization still occurred, necessitating the use of a photoabsorber. Azo dyes have been utilized as effective photoabsorbers to absorb reflected light and light bleed from the projected image,[28−30] and Oil Red O at a loading of 0.02% by mass was used to mitigate overpolymerization. The working curves of resins were measured for formulations at two printer irradiance levels to find ideal printing parameters. A working curve is a plot of cure depth (C_d) *versus* light dose (E_0). On a semilog plot, this graph returns a slope correlated to the light penetration into the resin (D_p) and the x-intercept is the critical light dose (E_c) required to form a gelled network.[31] These working curves and the extracted parameters are shown in Figure 5, along with UV−vis spectra of the resins.

Optically, the D_p extracted from the Jacobs equation[32] should correlate well with the D_p implied by the absorbance of the resin as measured in a UV−vis spectrophotometer. Figure 5 shows the extrapolated D_p values from the working curve along with the implied D_p values at 405 nm from the UV−vis data. The D_p values differ by several hundred micrometers, which implies that one of the fundamental assumptions made in a working curve (negligible consumption of photoinitiator and cessation of polymerization upon end of light exposure) is invalid for this resin system. The semilog plots shown in Figure 5a are quite linear, suggesting that there is no significant consumption of photoinitiator (*i.e.*, photobleaching) during the working curve measurement.[33−35] Lack of photobleaching suggests that the deviation from the working curve and UV−vis D_p values is due to "dark" polymerization. Early attempts to print these resins exhibited extensive weakly polymerized gel-like material that would form several millimeters outside of the patterned area (Figure S6, Supporting Information), suggesting that the reaction occurs even in the absence of light. This "dark polymerization" could explain the discrepancy between the working curve D_p and the UV−vis D_p, as the cured pillars used to measure the working curve would continue growing after the end of irradiation by the printer and as slides with resin were allowed to sit for several minutes prior to cleaning and measurement. The relative oxygen insensitivity of thiol−ene polymerization as compared to more conventional acrylate chemistry is hypothesized to explain this discrepancy: dissolved oxygen in an acrylate resin will lead to near-immediate termination of growing chain ends in the dark. The thiol−ene reaction is much less sensitive to oxygen and can continue in its presence, even after generation of new radicals has ceased after light exposure has stopped.[25,36] The observation of the weak gel and potential dark cure highlights the need to further refine this chemistry to lower the gel point (*i.e.*, E_c). Lower gel points would decrease layer times significantly and reduce or eliminate the opportunity for the weak gels to form. Elimination of the gels will also improve part resolution and surface finish.

Working curves for conventional acrylate-based resins measured in this manner previously led to successful prints at an energy dose corresponding to a ca. 4:1 theoretical/working curve C_d ratio (*i.e.*, a 100 μm layer would be printed with a dose that the working curve predicts to be ≈400 μm thick). This "overshooting" is attributed to the necessity of polymerizing the resin through the layer thickness and into the previous layer to develop sufficient strength to survive the lifting process. Optimal parameters for the 405 nm mUVe3D printer were determined to be a layer height of 100 μm, two burn-in layers at 50 s, and a layer exposure time of 20 s. This total energy dose of 140 mW cm^{-2} correlates to a theoretical layer thickness of ca. 570 μm from the Jacobs equation if it is assumed that the D_p from the UV−vis data and the E_c from the measured working curves are correct. Despite the presence of hypothesized dark polymerization, this is greater than the previous ca. 4:1 ratio. This could be due to a greater sensitivity of this resin to issues related to sufficient interlayer adhesion requiring higher doses than conventional resins, or due to the greater extent of reaction required for thiol−ene resins to reach gelation.[31] Lift height, peel speed, and retraction speed were found to be important for successful printing. Cylinders with a 30 mm diameter and 10 mm height were printed as proof-of-

https://doi.org/10.1021/acsapm.3c01601
ACS Appl. Polym. Mater. XXXX, XXX, XXX−XXX

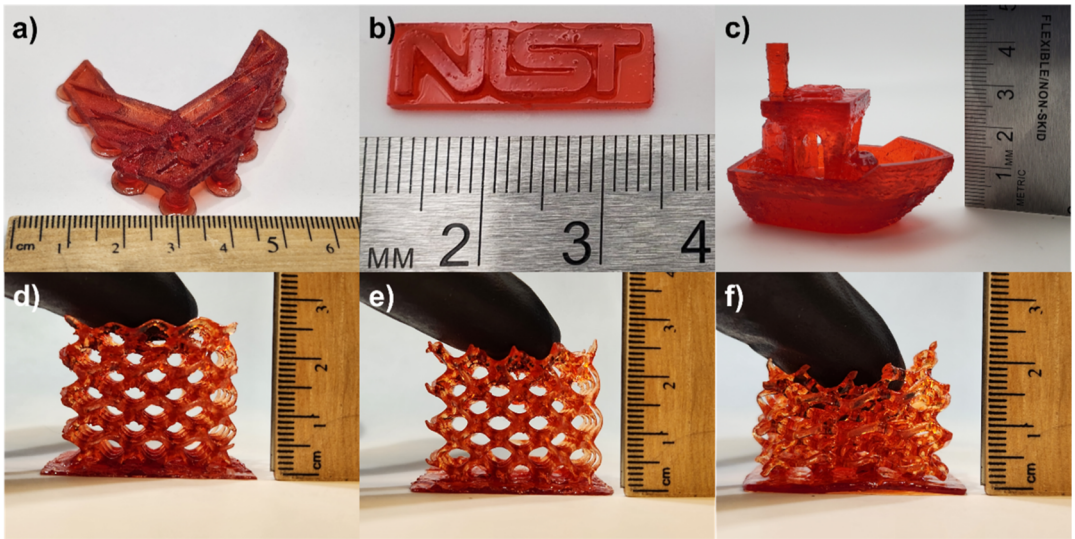

Figure 6. Complex geometries printed using the optimized resin based on PB resins and optimal printing parameters. A raw image of the United States Air Force symbol (a) printed from PB-5k/10SH before the supports were removed. Prints were also performed with the same PB-5k/10SH chemistry on a 30 mW cm^{-2} printer including the NIST logo (b) and Benchy (c). Lattice structures were printed on a 7 mW cm^{-2} printer with resin based on PB-5k (d), PB-8k (e), and PB-26k (f). Deformation was applied to each structure with the same perceived tactile force, and the original shape was recovered after the removal of force.

concept 3D parts, and optimal parameters were found to be a 5 mm lift height with a 0.25 mm s^{-1} peel speed, a 500 ms pause to allow the resin to recoat the bottom of the vat, and a 1 mm s^{-1} retraction speed.

Figure 6a–c shows complex geometries printed by using the PB-5k/10SH resin. To demonstrate the ability to print challenging structures such as overhanging features with this resin, the United States Air Force symbol was printed at an angle with supports on the back of the flat model using a 7 mW cm^{-2} printer (Figure 6a). This also shows the robustness of this chemistry to stand up to the forces generated during the printing process. The National Institute of Standards and Technology logo and a benchmark print known as "Benchy" (Figure 6b,, respectively) were printed by using a 30 mW cm^{-2} Asiga printer with the same PB-5k/10SH formulation, using the working curve as a guide to optimize parameters. Benchy is a common test print due to it possessing challenging overhanging features that are a key requirement of most AM technologies. Additionally, Benchy shows that this resin, even with the hypothesized dark polymerization, can be used to print negative-space features (*e.g.*, the cabin of the ship). Finally, a complex lattice structure was printed by using resins based on each prepolymer's 10SH/chain resin (Figure 6d–f). The resin based on PB-26k required plasticizer [bis(2-ethylhexyl)adipate] to reduce the viscosity to a printable level, as well as extended layer cure times (50 s), attributed to the relatively low amount of cross-linker in the formulation. The lattice prints show the ability to fabricate complex structures with varying bulk, and geometrically induced mechanical responses.

4. CONCLUSIONS

Unmodified liquid PB polymers were utilized to print complex geometries using DLP 3D printing by harnessing the inherent reactivity of the polymer's backbone as a substrate for thiol–ene cross-linking chemistry. An aliphatic dithiol was found to preferentially react with the pendent 1,2-vinyl and 1,4-*cis* moieties of the polymer over the 1,4-*trans* moiety, with the 1,2-vinyl moiety being most reactive. These reactive handles were then utilized as cross-linking sites when cured with an aliphatic dithiol in the UV-promoted thiol–ene click reaction. Photopolymer resins were prepared using varied prepolymer molecular weights and dithiol cross-linker loadings, and their mechanical properties generally followed the expected trends wherein higher molecular weight between cross-links led to a cured material with higher strain at break and lower UTS. Working curves were prepared in a printer, at different irradiance outputs, and the resultant depths of light penetration differed consistently from measurements made with UV–vis. This difference was attributed to dark polymerization, which is characteristic of thiol–ene reactions. Complex geometries were printed in two separate laboratories in different DLP printers, showing the generalizability of the formulations. Overall, this effort expands the available materials toolbox for VP of elastomers, a commercially important but underexplored material class within AM.

■ ASSOCIATED CONTENT

Supporting Information

The Supporting Information is available free of charge at https://pubs.acs.org/doi/10.1021/acsapm.3c01601.

FTIR spectra, detailed ^{1}H NMR spectra, detailed resin formulations, and photographs of preliminary prints (PDF)

■ AUTHOR INFORMATION

Corresponding Author

Levi M. J. Moore – *Aerospace Systems Directorate, Air Force Research Laboratory, Edwards Air Force Base, California 93524, United States;* orcid.org/0000-0002-8010-4795; Email: levi.moore.1@us.af.mil

Authors

Van Michael Q. Saludo – *Aerospace Systems Directorate, Air Force Research Laboratory, Edwards Air Force Base, California 93524, United States*

Oliver H. Grasdal − *Department of Chemistry, United States Air Force Academy, Colorado Springs, Colorado 80840, United States*
Kayleen M. Smith − *Aerospace Systems Directorate, Air Force Research Laboratory, Edwards Air Force Base, California 93524, United States*
Thomas J. Kolibaba − *Applied Chemicals and Materials Division, National Institute of Standards and Technology, Boulder, Colorado 80305, United States*
Jacob C. Marcischak − *Aerospace Systems Directorate, Air Force Research Laboratory, Edwards Air Force Base, California 93524, United States*
Jason P. Killgore − *Applied Chemicals and Materials Division, National Institute of Standards and Technology, Boulder, Colorado 80305, United States;* orcid.org/0000-0002-8458-6680
Jeremy J. Snyder − *Exquadrum, Inc., Air Force Research Laboratory, Edwards Air Force Base, California 93524, United States*
Gregory R. Yandek − *Aerospace Systems Directorate, Air Force Research Laboratory, Edwards Air Force Base, California 93524, United States*
Kamran B. Ghiassi − *Aerospace Systems Directorate, Air Force Research Laboratory, Edwards Air Force Base, California 93524, United States;* orcid.org/0000-0002-3557-2813

Complete contact information is available at: https://pubs.acs.org/10.1021/acsapm.3c01601

Notes

The authors declare no competing financial interest.

ACKNOWLEDGMENTS

The authors gratefully acknowledge support from the Air Force Office of Scientific Research, and from the Air Force Research Laboratory, Aerospace Systems Directorate. This work was performed while Thomas Kolibaba held a National Research Council Associateship Award at the National Institute of Standards and Technology (NIST). Certain commercial equipment, instruments, or materials are identified in this paper to specify the experimental procedure adequately. Such identification is not intended to imply recommendation or endorsement by the USAF or NIST.

REFERENCES

(1) Xiao, J.; Gao, Y. The manufacture of 3D printing of medical grade TPU. *Prog. Addit. Manuf.* **2017**, *2* (3), 117−123.
(2) Gama, N.; Ferreira, A.; Barros-Timmons, A. 3D Printed Thermoplastic Polyurethane Filled with Polyurethane Foams Residues. *J. Polym. Environ.* **2020**, *28* (5), 1560−1570.
(3) Kazmer, D. O.; Kodra, S.; Mubasshir, A. A.; Keaney, E. E.; Mead, J. L. Additive ram material extrusion and diddling of fully compounded thermoset nitrile rubber. *Polym. Compos.* **2021**, *42* (10), 5237−5248.
(4) Herzberger, J.; Sirrine, J. M.; Williams, C. B.; Long, T. E. Polymer Design for 3D Printing Elastomers: Recent Advances in Structure, Properties, and Printing. *Prog. Polym. Sci.* **2019**, *97*, 101144.
(5) Scott, P. J.; Meenakshisundaram, V.; Hegde, M.; Kasprzak, C. R.; Winkler, C. R.; Feller, K. D.; Williams, C. B.; Long, T. E. 3D Printing Latex: A Route to Complex Geometries of High Molecular Weight Polymers. *ACS Appl. Mater. Interfaces* **2020**, *12* (9), 10918−10928.
(6) Zhao, T.; Yu, R.; Li, S.; Li, X.; Zhang, Y.; Yang, X.; Zhao, X.; Wang, C.; Liu, Z.; Dou, R.; Huang, W. Superstretchable and Processable Silicone Elastomers by Digital Light Processing 3D Printing. *ACS Appl. Mater. Interfaces* **2019**, *11* (15), 14391−14398.
(7) Coran, A. Y. Chemistry of the vulcanization and protection of elastomers: A review of the achievements. *J. Appl. Polym. Sci.* **2003**, *87* (1), 24−30.
(8) Scott, P. J.; Meenakshisundaram, V.; Chartrain, N. A.; Sirrine, J. M.; Williams, C. B.; Long, T. E. Additive Manufacturing of Hydrocarbon Elastomers via Simultaneous Chain Extension and Cross-linking of Hydrogenated Polybutadiene. *ACS Appl. Polym. Mater.* **2019**, *1* (4), 684−690.
(9) Maurya, S. D.; Kurmvanshi, S. K.; Mohanty, S.; Nayak, S. K. A Review on Acrylate-Terminated Urethane Oligomers and Polymers: Synthesis and Applications. *Polym.-Plast. Technol. Eng.* **2018**, *57*, 625−656.
(10) ten Brummelhuis, N.; Diehl, C.; Schlaad, H. Thiol-Ene Modification of 1,2-Polybutadiene Using UV Light or Sunlight. *Macromolecules* **2008**, *41* (24), 9946−9947.
(11) Decker, C.; Nguyen Thi Viet, T. Photocrosslinking of functionalized rubbers IX. Thiol-ene polymerization of styrene-butadiene-block-copolymers. *Polymer* **2000**, *41* (11), 3905−3912.
(12) Nakazono, T.; Matsumoto, A. Mechanical properties and thermal aging behavior of styrene-butadiene rubbers vulcanized using liquid diene polymers as the plasticizer. *J. Appl. Polym. Sci.* **2010**, *118* (4), 2314−2320.
(13) Kuraray Elastomer Product Brochure. https://www.elastomer.kuraray.com/us/wp-content/uploads/sites/2/2021/07/Kuraray-Elastomer-Product-Brochures-Kuraray-Liquid-Rubber.pdf (accessed March 21, 2023).
(14) Mondschein, R. J.; Kanitkar, A.; Williams, C. B.; Verbridge, S. S.; Long, T. E. Polymer structure-property requirements for stereolithographic 3D printing of soft tissue engineering scaffolds. *Biomaterials* **2017**, *140*, 170−188.
(15) Strohmeier, L.; Frommwald, H.; Schlögl, S. Digital light processing 3D printing of modified liquid isoprene rubber using thiol-click chemistry. *RSC Adv.* **2020**, *10* (40), 23607−23614.
(16) Bragaglia, M.; Lamastra, F. R.; Cherubini, V.; Nanni, F. 3D printing of polybutadiene rubber cured by photo-induced thiol-ene chemistry: A proof of concept. *Express Polym. Lett.* **2020**, *14*, 576−582.
(17) Kolibaba, T. J.; Higgins, C. I.; Crawford, N. C.; Samaniuk, J. R.; Killgore, J. P. Sustainable Additive Manufacturing of Polyelectrolyte Photopolymer Complexes. *Adv. Mater. Technol.* **2023**, *8*, 2201681.
(18) Behera, P. K.; Mandal, P.; Maiti, M.; Jasra, R. V.; Singha, N. K. Insights into the Preparation of Vinyl Polybutadiene Via Cobalt-Based Catalyst: Tuning Its Properties by Thiol-Ene Modification of Vinyl Group. *Rubber Chem. Technol.* **2016**, *89* (2), 335−348.
(19) Vitale, A.; Massaglia, G.; Chiodoni, A.; Bongiovanni, R.; Pirri, C. F.; Quaglio, M. Tuning Porosity and Functionality of Electrospun Rubber Nanofiber Mats by Photo-Crosslinking. *ACS Appl. Mater. Interfaces* **2019**, *11* (27), 24544−24551.
(20) Liu, Y.; Yuan, Y.; Liu, J.; Hua, J. High wear-resisting,superhydrophobic coating with well aging resistance and ultrahigh corrosion resistant on high vinyl polybutadiene rubber substrate by thiol-ene click chemistry. *Polym. Test.* **2021**, *101*, 107312.
(21) Roper, T. M.; Guymon, C. A.; Jönsson, E. S.; Hoyle, C. E. Influence of the alkene structure on the mechanism and kinetics of thiol-alkene photopolymerizations with real-time infrared spectroscopy. *J. Polym. Sci., Part A: Polym. Chem.* **2004**, *42* (24), 6283−6298.
(22) Liu, X.; Zhou, T.; Liu, Y.; Zhang, A.; Yuan, C.; Zhang, W. Cross-linking process of cis-polybutadiene rubber with peroxides studied by two-dimensional infrared correlation spectroscopy: a detailed tracking. *RSC Adv.* **2015**, *5* (14), 10231−10242.
(23) Chatgilialoglu, C.; Ferreri, C. Trans Lipids: The Free Radical Path. *Acc. Chem. Res.* **2005**, *38* (6), 441−448.
(24) Haddad, T. S.; Moore, L. M. J.; Reams, J. T.; Ford, M. D.; Marcischak, J. C.; Guenthner, A. J.; Mabry, J. M.; Ghiassi, K. B. NMR Analysis of Hydroxyl-Terminated Polybutadiene End Groups and Reactivity Differences with Monoisocyanates. *J. Polym. Sci., Part A: Polym. Chem.* **2018**, *56* (23), 2665−2671.
(25) Hoyle, C. E.; Bowman, C. N. Thiol-Ene Click Chemistry. *Angew. Chem., Int. Ed.* **2010**, *49* (9), 1540−1573.

(26) Van Damme, J.; van den Berg, O.; Brancart, J.; Vlaminck, L.; Huyck, C.; Van Assche, G.; Van Mele, B.; Du Prez, F. Anthracene-Based Thiol-Ene Networks with Thermo-Degradable and Photo-Reversible Properties. *Macromolecules* **2017**, *50* (5), 1930−1938.
(27) Bijarimi, M.; Zulkafli, H.; Beg, M. D. H. Mechanical Properties of Industrial Tyre Rubber Compounds. *J. Appl. Sci.* **2010**, *10*, 1345−1348.
(28) Li, V. C.-F.; Kuang, X.; Mulyadi, A.; Hamel, C. M.; Deng, Y.; Qi, H. J. 3D printed cellulose nanocrystal composites through digital light processing. *Cellulose* **2019**, *26* (6), 3973−3985.
(29) Kuang, X.; Wu, J.; Chen, K.; Zhao, Z.; Ding, Z.; Hu, F.; Fang, D.; Qi, H. J. Grayscale digital light processing 3D printing for highly functionally graded materials. *Sci. Adv.* **2019**, *5* (5), No. eaav5790.
(30) Wang, X.; Schmidt, F.; Hanaor, D.; Kamm, P. H.; Li, S.; Gurlo, A. Additive manufacturing of ceramics from preceramic polymers: A versatile stereolithographic approach assisted by thiol-ene click chemistry. *Addit. Manuf.* **2019**, *27*, 80−90.
(31) Schwartz, J. J. Additive manufacturing: Frameworks for chemical understanding and advancement in vat photopolymerization. *MRS Bull.* **2022**, *47* (6), 628−641.
(32) Jacobs, P. F. *Rapid Prototyping & Manufacturing: Fundamentals of Stereolithography*; Society of Manufacturing Engineers, 1992.
(33) Kenning, N. S.; Ficek, B. A.; Hoppe, C. C.; Scranton, A. B. Spatial and temporal evolution of the photoinitiation rate for thick polymer systems illuminated by polychromatic light: selection of efficient photoinitiators for LED or mercury lamps. *Polym. Int.* **2008**, *57* (10), 1134−1140.
(34) Bennett, J. Measuring UV curing parameters of commercial photopolymers used in additive manufacturing. *Addit. Manuf.* **2017**, *18*, 203−212.
(35) Rau, D. A.; Reynolds, J. P.; Bryant, J. S.; Bortner, M. J.; Williams, C. B. A rheological approach for measuring cure depth of filled and unfilled photopolymers at additive manufacturing relevant length scales. *Addit. Manuf.* **2022**, *60*, 103207.
(36) Black, M.; Rawlins, J. W. Thiol-ene UV-curable coatings using vegetable oil macromonomers. *Eur. Polym. J.* **2009**, *45* (5), 1433−1441.

https://doi.org/10.1021/acsapm.3c01601
ACS Appl. Polym. Mater. XXXX, XXX, XXX−XXX